

Adaptive Transmission Rate for LQG Control over Wi-Fi: a Cross-Layer Approach [★]

Matthias Pezzutto ^a, Federico Tramarin ^b, Subhrakanti Dey ^c, Luca Schenato ^a

^a*Department of Information Engineering, University of Padova, Padova, Italy*

^b*Enzo Ferrari Engineering Department, University of Modena and Reggio Emilia, Modena, Italy*

^c*Hamilton Institute, National University of Ireland, Maynooth, County Kildare, Ireland*

Abstract

This work studies the problem of LQG control when the link between the sensor and the controller relies on a Wi-Fi network. Unfortunately, the communication on a wireless medium is sensitive to noise in the transmission band, which is characterized by the Signal-to-Noise Ratio (SNR). Wi-Fi allows to switch among different bit-rates in real-time thus permitting to trade-off lower loss probabilities for larger latency or vice-versa to achieve better closed-loop performance. To exploit this feature, under a constant SNR scenario, we propose a cross-layer approach where the bit-rate is optimally selected based on a control performance metric (i.e. minimum LQG cost) and a model-based controller is used to compensate for the packet losses. Under time-varying SNR, we additionally propose a (sub-optimal) on-line rate adaptation strategy and we guarantee the closed-loop stability under some mild conditions. Numerical comparisons with emulation-based approaches using TrueTime, a realistic Matlab-based Wi-Fi simulator, are included to show the benefits of the adaptive approach under time-varying SNR scenarios.

Key words: Wi-Fi; Rate selection; LQG; Control over wireless; Packet loss.

1 Introduction

Motivated by the flexibility required by multi-agent or distributed systems, as well as the reduction of installation and maintenance costs, wireless Networked Control Systems (NCSs) have attracted the interest of the control community in the past two decades. As surveyed in e.g [26], many ad-hoc algorithms and strategies have been proposed to overcome the stochastic delays and random packet loss typically affecting wireless NCSs. As for the communication protocol, from an industrial perspective, wireless standards such as WirelessHART [11] and ISA100.11a [14] have been specifically designed for control applications aiming to enforce deterministic delays, while minimizing both the packet loss probability and the energy consumption of the devices. The available data-rate is nevertheless very low, i.e. 250 kbit/s over a time-slotted channel with a minimum time slot duration of 10 ms. Due to such low data-rate and communication overheads, they do not allow sampling periods smaller

than approximately 50 ms [27]. In order to control systems with higher control rate, but also to share the network among several systems, the required higher data-rates can be provided by the IEEE 802.11 standards, usually known as Wi-Fi. Under very good channel conditions, rates up to 150 Mbit/s (excluding multiple spatial streams) are provided by IEEE 802.11n standard, and more recent releases allow even higher rates. Motivated by this attractive feature, a preliminary attempt to investigate the use of Wi-Fi for industrial automation application is provided in [35], where the effects of different parameters such as retransmission number and back-off delay are examined in terms of losses and latencies, while [37] proposes the custom RT-WiFi protocol to enhance the timing performance by changing the medium access mechanism. On the other hand, the main drawback of Wi-Fi is that, as well as other wireless standards, the channel can be affected by external disturbances and suffer from interference from other networks operating on the same band. How much the external disturbance level, quantified by the Signal-to-Noise Ratio (SNR), affects the communication is related to the adopted modulation. Indeed, higher data-rates exploit noise-sensitive high-order modulations, hence allowing to send the same amount of data in a smaller period at the price of a

[★] This paper was not presented at any IFAC meeting. This work is partially supported by University of Padova, project MAGIC SCHE_SID17_01. Corresponding author: Matthias Pezzutto, mail: matthias.pezzutto@phd.unipd.it.

greater number of corrupted (i.e. lost) packets. On the other hand, lower data-rates ensure lower loss probabilities in bad channel conditions thanks to their robust modulations. Wi-Fi standard allows to choose the data-rate in real-time but which rate should be chosen is not obvious since it depends on the desired applications and whether these are time-critical or not. The first possible approach, adopted by most off-the-shelf devices, prescribes to choose the data-rate in view of the overall throughput of the network at the cost of unpredictable and possibly long delays. In this sense, well-known algorithms are the Automatic Rate Fallback [15], the Adaptive Automatic Rate Fallback [17], and the SNR-based Receiver Based Auto Rate [13]. An exhaustive overview is presented in [3]. However, they are not suitable for control and safety-critical applications, where the lack of information for a certain period can be dangerous and it is generally deprecated. This has motivated rate selection algorithms tailored for control applications, and also in this particular case different approaches exist. First, there exist algorithms that choose the data-rate according to a communication metric that is supposed to affect the control. In industrial scenario, a good example is the Minstrel algorithm [38], that prescribes to follow a sequence of data-rates from a set of four chosen according to the throughput and the estimated packet loss probability. The authors of [36] propose two algorithms, which increase and decrease the data-rate after a series of successful or failed transmissions, while always retransmitting at the lowest data-rate. The work [34] proposes to find a sequence of data-rates in order to minimize the residual packet loss probability based on the current estimated SNR. However, all these algorithms admit multiple retransmissions of the same measurement that, while decreasing the loss probability, entail the transmission of already outdated information. In the same line, another example is [7], where authors investigate how to change on-line the sampling rate (which often coincides with the transmission packet-rate) as a function of the round-trip delay. A second field of research (see [22] and the reference therein) has handled the minimum bit-rate required to stabilize a system. Finally, instead of considering a communication metric that affects the control or only the closed-loop stability, the third approach directly addresses the performance of the control. The resulting design is said to be cross-layer, since the data-rate, that is a communication parameter, is selected based on control performance. An approach along this line is proposed for IEEE 802.15.4 standard (which is at the core of Zigbee and WirelessHART) in [24], that studies how to choose the sampling rate and other communication parameters based on aspects of the control. In [29], the authors discuss optimal sampling rate strategies from a control perspective in a multi-hop sensor network. In our specific case, we devise an algorithm that selects the data-rate according to the LQG cost.

An important aspect of our work is the adoption of a update rate of the control input higher than the rate

at which the output is communicated. This type of systems, usually named dual-rate or multi-rate systems, have been studied since the 50s and several contributions have appeared since then: for example, parameter identification and the output estimation are treated in [21][10], the LQG problem is addressed in [18], while [20] studies modeling imperfections. Recent works e.g. [12] have applied multi-rate control systems to NCSs for their ability of decreasing the traffic load on the network. In our framework, the multi-rate configuration allows us to compute the optimal estimator/controller also with time-varying output sampling rate, while this is not possible with time-varying control rates.

The main contribution of this work is the simultaneous optimization of the control policy and transmission rate in a LQG framework. We assume that the packet loss and the delay are a function of the SNR level and of the transmission rate. First, under a constant SNR scenario, we find the joint optimal rate and LQG controller as a function of the SNR level. We find an explicit (tight) upper bound of the optimal LQG cost and we show the optimal loss probability for each SNR level. Then, we consider a more challenging scenario with a time-varying SNR, in which the joint optimization of the rate and the controller gain is computationally infeasible, and we propose to select the rate on a packet basis as if the current SNR would be constant. A preliminary version of this approach has been presented in [28], but this strategy was only numerically evaluated on a linear system. Here, we move forward: under the proposed (possibly sub-optimal) dynamic rate selection strategy, we show that the optimal LQG controller can still be computed in closed form. Moreover, we devise novel mathematical tools and determine sufficient conditions to prove stability for this dynamic multi-rate scenario with lossy communication. In fact, the time-varying nature of the SNR requires us to find bounds on the estimator error covariance that hold true simultaneously for possibly different values of the SNR, which is quite challenging in the presence of packet loss. Finally, we show the benefits of this approach with respect to alternative control strategies referred to as emulation-based [23][9], using a realistic Wi-Fi environment based on the TrueTime simulator [6].

The paper is organized as follows: in Sec. 2 we introduce our main assumptions, the network and the plant models; Sec. 3 shows the solution of the estimation problem and the jointly optimal rate and optimal control problem under constant SNR, while Sec. 4 outlines our rate selection algorithm; in Sec. 5 we address the time-varying SNR case and we prove the stability in this general case. The paper ends with simulations and the conclusions.

2 Problem formulation

The following two definitions are widely used in the rest of the paper.

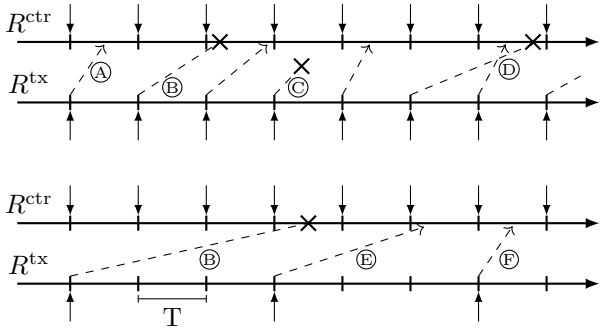


Fig. 1. Control instants and transmission instants with R_1 (above) and R_3 (below). When sent, a packet can arrive on time (A), be outdated and discarded (B), or lost (C). Out-of-order delivers are detected (D). A measure is used to update the estimate and the control input as soon as possible: e.g. after $3T$ (E) or after T (F). Transmitter and receiver are assumed to be synchronized, and packets are time-stamped.

Definition 1 The control rate R^{ctr} is the inverse of the sampling period to which the system is discretized. It corresponds to the rate at which the input and the estimate are updated. The transmission rate R^{tx} is the inverse of the period between two consecutive transmitted measurements. It corresponds to the rate at which the output is sampled and communicated.

We consider the set of periods T_i $i \in \{1, 2, \dots, M\}$, which represent both the sampling periods and the periods between two transmissions. For sake of simplicity, we assume that $T_i = i \cdot T_1$. The smallest period is simply indicated by T , so the set of given periods is $\{T, 2T, \dots, MT\}$. From the relation $R_i = 1/T_i$, it is possible to derive the set of rates R_i $i \in \{1, 2, \dots, M\}$; it holds that $R_i = R_1/i$. The transmission period and the control period can be the same (top panel in Fig. 1), but in general the former is a multiple of the latter if the bit-rate is reduced (bottom panel in Fig. 1).

To avoid confusion it is important to remark that transmission rates in this work are defined in terms of *packets/s* and should not be confused with data-rates which are in *bits/s*. Although they are not exactly proportional, we associate different transmission rates to different data-rates in such a way that a higher transmission rate is associated to a higher data-rate, and a lower transmission rate to a lower data-rate.

2.1 Communication

We consider to connect the sensor and the estimator through a Wi-Fi network. Our work does not employ a detailed network model, but it relies on a simplified formulation whose main assumptions are introduced in the following.

Assumption 2 Each packet is delivered within the following transmission instant with a certain packet arrival

probability λ which depends on the transmission rate and on the SNR level:

$$\lambda(R^{\text{tx}}, \text{SNR}). \quad (1)$$

The transmission delay for successfully delivered packets is assumed to be uniformly distributed across the transmission period. Additionally, assume that receiver and transmitter are synchronized, and that packets are time-stamped.

The previous assumption requires that the arrival probability is only a function of the SNR and of the transmission rate. In the context of NCSs, similar ideas have been previously proposed based on the Gilbert-Elliot model or Markov chains, for example, to represent the relation between the quality of the channel and arrival probability. A more sophisticated framework have been considered in [25], where also network parameters are taken into account. In this work, based on known communication principles [33], we consider that for a given R^{tx} , the function $\lambda(R^{\text{tx}}, \text{SNR})$ is monotonically non decreasing with respect to the SNR. On the other hand, for a given SNR level, a lower transmission rate R^{tx} achieves higher arrival probability λ because the associated data-rate adopts a more robust modulation. Accordingly, we refer to the packet loss probability $1 - \lambda$ as the probability with which the packet does not arrive before the following transmission instant. In that case, the packet is discarded. Uniform delays across the transmission period are assumed for sake of simplicity, but the subsequent analysis can be easily generalized to any other delay distribution. Out-of-order and outdated packets are detected since receiver and transmitter are synchronized and packets are time-stamped. An illustrative scheme is reported in Fig. 1. Note that the period between two consecutive transmission instants, and hence the allowed delay, is different for each transmission rate.

Curves of packet loss probability vs SNR can be inferred analytically or empirically, see for example [36] [16], and depend on the number of retransmissions, the payload, and the traffic load, i.e. on the particular application. In this work we consider that packets have a fixed length, we disable retransmissions, and we consider load condition such to have the curves shown in Fig. 2, derived from [36] for IEEE 802.11g. Nevertheless, our theoretical procedure can be applied regardless to the specific curve, i.e. for different network configurations and for different IEEE 802.11 or other standards that allow the selection of the transmission rate in real-time.

2.2 System dynamics

Consider the stochastic continuous-time linear system:

$$\begin{cases} dx(t) = A_c x(t) dt + B_c u(t) dt + dw(t) \\ y(t) = C_c x(t) \end{cases} \quad (2)$$

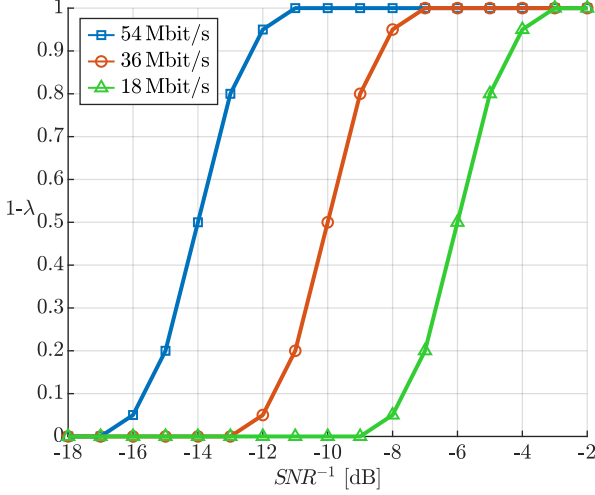


Fig. 2. Curves of loss probability vs SNR.

where $x(t) \in \mathbb{R}^n$, $y(t) \in \mathbb{R}^p$, $u(t) \in \mathbb{R}^m$, and $w(t) \in \mathbb{R}^n$ is a Wiener process such that $w(t+\tau) - w(t) \sim \mathcal{N}(0, Q_c\tau)$, $Q_c \geq 0$, where $\mathcal{N}(\cdot)$ indicates a Gaussian distribution.

Consider to control the system with a NCS. The controller and the estimator are implemented on the same device. At each transmission instant, the sensor transmits a packet containing the current output to the estimator through a Wi-Fi network, while, at each sampling instant, the controller updates and transmits the input to the actuator through an ideal link. This configuration corresponds to the very common situation in which the controller and the actuator are co-located. The sensor, the estimator, the controller, and the actuator need to be synchronized and the packets have to be time-stamped as stated in Assumption 2. The scheme is reported in Fig. 3.

To deal with this set-up, we consider piecewise constant inputs within a sampling period T_i $i \in \{1, 2, \dots, M\}$, i.e. $u(t) = u_k$, $t \in [kT_i, (k+1)T_i)$. Under this scenario, the continuous system (2) can be discretized following [19] as:

$$\begin{cases} x_{k+1} = A_i x_k + B_i u_k + w_k \\ y_k = C_i x_k + v_k \end{cases}$$

where $x_k := x(kT_i)$, $y_k := y(kT_i)$, $w_k \sim \mathcal{N}(0, Q(T_i))$, $v_k \sim \mathcal{N}(0, R)$ with $R > 0$, and $A_i = A(T_i)$, $B_i = B(T_i)$, $C_i = C_c$ where:

$$A(\tau) = e^{A_c\tau}; \quad B(\tau) = \int_0^\tau e^{A_c t} B_c dt; \quad Q(\tau) = \int_0^\tau e^{A_c t} Q_c e^{A_c t} dt.$$

We assume that the process noise w_k is independent of the measurement noise v_k . The measurement noise covariance matrix R is assumed to be independent of the sampling period. We finally assume that the initial state is a Gaussian random vector with mean \hat{x}_0 and covariance matrix P_0 . Define the measurement model at

the estimator as:

$$y_h^k = \gamma_h^k y_h = \gamma_h^k (C_i x_h + v_h)$$

where the arrival process $\gamma_h^k \in \{0, 1\}$ indicates if the measurement y_h sampled at time hT_i has been present at the estimator location at time $kT_i > hT_i$. In the following, to simplify the notation, if $i = 1$ we omit it, so: $A := A_1$, $B := B_1$, $C := C_1$, and $Q := Q_1$.

2.3 LQG cost

Consider the following quadratic cost measure:

$$J_M(u(t)) = \mathbb{E} \left[\frac{1}{M} \int_0^M (x'(t) W_c x(t) + u'(t) U_c u(t)) dt \mid u(t), t \in [0, M] \right]$$

with $W_c \geq 0$ and $U_c > 0$. Under the assumption of piecewise constant inputs over T , similarly to [8], the previous integral can be converted into the following sum:

$$J_K(u_k) = c + \mathbb{E} \left[\frac{1}{K} \sum_{k=0}^{K-1} x'_k W x_k + 2x'_k N u_k + u'_k U u_k \mid \{u_k\}_{k=0}^{K-1} \right]$$

where $J_M(u(t)) = J_K(u_k)$ with $K := \frac{M}{T}$ and

$$W = \frac{1}{T} \int_0^T A'(\tau) W_c A(\tau) d\tau \quad N = \frac{1}{T} \int_0^T A'(\tau) W_c B(\tau) d\tau \\ U = U_c + \frac{1}{T} \int_0^T B'(\tau) W_c B(\tau) d\tau \quad c = \frac{1}{T} \int_0^T \text{tr}(Q(\tau) W_c) d\tau.$$

In the following sections, we will need the operator:

$$g_\lambda^{T_i}(X) := A_i X A_i' + Q_i - \lambda A_i X C_i' (C_i X C_i' + R)^{-1} C_i X A_i'$$

with T_i the sampling period of the system. We also define the critical arrival probability $\bar{\lambda}_i$ similarly to [32]:

$$\bar{\lambda}_i = \arg \inf \left\{ \lambda : \exists X \geq 0 \text{ s.t. } g_\lambda^{T_i}(X) = X \right\}.$$

3 LQG control under constant SNR

In this section, we introduce the LQG control in a scenario where the control rate is fixed to the highest rate, i.e. $R^{\text{ctr}} = R_1$, while the transmission rate R^{tx} is fixed but is chosen in the set $R^{\text{tx}} \in \{R_1, \frac{R_1}{2}, \dots, \frac{R_1}{M}\}$, with outputs randomly lost according to an i.i.d. process with arrival probability λ defined in (1). The resulting control strategy is therefore named *Single-Rate Controller*

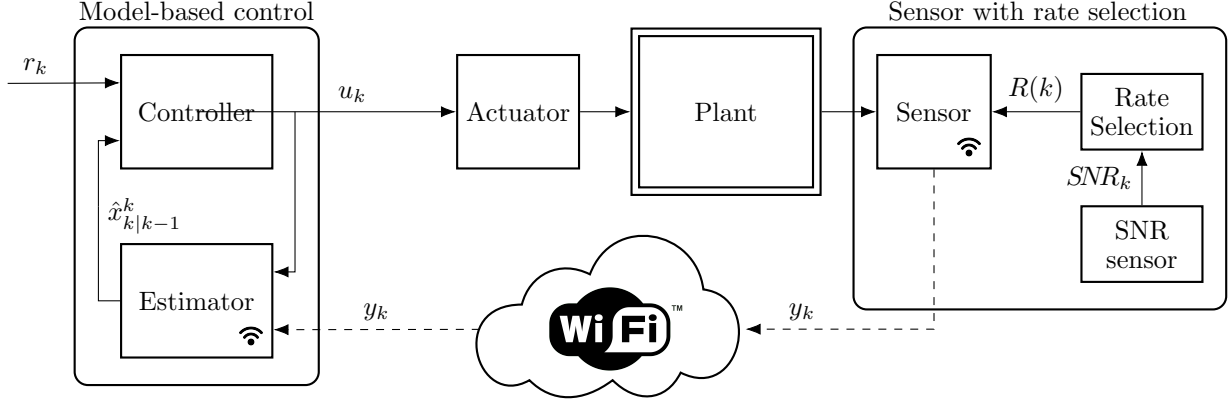


Fig. 3. Control and rate selection architecture

(SRC). This choice arises from the different nature of the two links: while a high control rate is supported by the ideal link between the controller and the actuator, a high transmission rate requires good channel conditions in the wireless connection between the sensor and the controller. We further assume that the SNR is constant, from which it follows that the arrival probability depends only on R^{tx} according to (1).

Consider $u(t) = u_k, t \in [kT, (k+1)T)$, where $T = 1/R_1$. We define the information set \mathcal{I}_k , that is the information available at the controller/estimator at time instant k :

$$\mathcal{I}_k = \{ \{y_h^k\}_{h=0}^{k-1}, \{\gamma_h^k\}_{h=0}^{k-1}, \{u_h\}_{h=0}^{k-1} \}.$$

Note that at time instant k the measurement y_k is not available, since we assume a non-zero transmission delay to send it over the network (see Fig. 1). The information set implicitly depends on the SNR and on R^{tx} since the arrival process is highly affected by them. We define the following variables:

$$\begin{aligned} \hat{x}_{t|t-1}^k &:= \mathbb{E}[x_t | \mathcal{I}_k] \\ P_{t|t-1}^k &:= \mathbb{E}[(x_t - \hat{x}_{t|t-1}^k)(x_t - \hat{x}_{t|t-1}^k)' | \mathcal{I}_k]. \end{aligned}$$

Since initial state, process noise, and measurement noise are independent and Gaussian, $\hat{x}_{t|t-1}^k$ is the optimal estimator given \mathcal{I}_k [1], and the matrix $P_{t|t-1}^k$ denotes the corresponding estimation error covariance matrix. With delayed packets, the optimal estimator can be found following [30]:

$$\hat{x}_{t|t-1}^k = A\hat{x}_{t-1|t-2}^k + Bu_{t-1} + \gamma_{t-1}^k K_{t-1}^k (y_{t-1}^k - C\hat{x}_{t-1|t-2}^k) \quad (3)$$

$$K_{t-1}^k = AP_{t-1|t-2}^k C' (CP_{t-1|t-2}^k C' + R)^{-1} \quad (4)$$

$$P_{t|t-1}^k = AP_{t-1|t-2}^k A' + Q - \gamma_{t-1}^k K_{t-1}^k CP_{t-1|t-2}^k A' \quad (5)$$

for each t in $[0, k]$. The optimal estimator is time-varying and depends on the particular realization of the packet arrival process γ_{t-1}^k , which in turn depends on R^{tx} . The

estimate is updated according to an open-loop estimation if $\gamma_{t-1}^k = 0$ and to a Kalman (closed-loop) update if $\gamma_{t-1}^k = 1$. In our framework we have assumed that a measurement arrives within the following transmission instant or it never arrives. Since the period between two consecutive transmissions contains $R^{\text{ctr}}/R^{\text{tx}}$ sampling periods, a measurement can arrive with a delay up to $R^{\text{ctr}}/R^{\text{tx}}$ control periods. This requires to store the estimate and the error covariance of the previous transmission instant and at each step to repeat the estimation procedure from that instant to the current instant. This allows to improve the performance of the estimation in the interval between two transmission instants: instead of using the previous transmitted output at the following transmission instant, it can be used on the intermediate instants, if it is available (see bottom panel of Fig. 1).

Now consider the following finite-horizon optimization problem:

$$J_K^*(\{\gamma_t^k\}) := \underset{\{u_k\}_{k=0}^{K-1}}{\operatorname{argmin}} J_K(u_k), \quad \text{s.t. } u_k = f_k(\mathcal{I}_k) \quad (6)$$

where we made explicit that the optimal cost depends on the specific packet arrival sequence $\{\gamma_t^k\}$. The following theorem solves this problem.

Theorem 3 Consider the continuous system (2) with control rate $R^{\text{ctr}} = R_1$. Consider the finite-horizon LQG problem (6). Then, the optimal solution is given by:

$$\begin{aligned} J_K^*(\{\gamma_t^k\}) &= c + \frac{1}{K} \left(\hat{x}'_0 S_0 \hat{x}_0 + \operatorname{tr}(S_0 P_0) + \right. \\ &\quad \left. + \sum_{k=0}^{K-1} \operatorname{tr}(S_{k+1} Q) + \operatorname{tr} \left((A' S_{k+1} A + W - S_k) P_{k|k-1}^k \right) \right) \end{aligned}$$

with

$$\begin{aligned} u_k &= L_k \hat{x}_{k|k-1}^k \\ L_k &= -(U + B' S_{k+1} B)^{-1} (B' S_{k+1} A + N') \\ S_k &= A' S_{k+1} A + W - (A' S_{k+1} B + N) L_k \quad S_K = 0 \end{aligned}$$

while the optimal estimator is given in (3)-(5).

The proof of the previous theorem is omitted since it follows from a straightforward readjustment of the proof of Lemma 5.1 in [31] by including the cross cost term N in the cost. In this way it is possible to show that the separation principle holds and the optimal estimator can be solved separately. Moreover since the optimal control gains L_k are independent of the transmission arrival sequence $\{\gamma_t^k\}$, then it means that they are independent of the specific transmission rate R^{tx} and of the SNR, thus can be computed off-line. This is a specific feature of the SRC approach. In fact, if the control rate would be chosen to be equal to the transmission rate, i.e. $R^{\text{ctr}} = R^{\text{tx}}$, then the control gains L_k would be different for different rates. While under the constant SNR scenario this is not critical since stability can still be guaranteed, in the time-varying scenario where transmission rate is changed on-line, this would require the switching of control gains thus leading to a possible unstable switching dynamics.

4 Optimal rate for constant SNR

Since the error covariance depends on the arrival process that is not known in advance, we consider the expected value of the cost with respect to the arrival process. We focus our attention on the infinite-horizon LQG problem. Under standard stabilizability of the pair (A, B) and detectability of the pair (A, \sqrt{W}) , with $\sqrt{W}'\sqrt{W} = W$, then $\lim_{k \rightarrow \infty} S_k = S_\infty$ exists, the control gain L_k converges to:

$$L_\infty = -(U + B' S_\infty B)^{-1} (B' S_\infty A + N') \quad (7)$$

and the cost evaluated on the optimal input is:

$$\begin{aligned} J_\infty^*(R^{\text{tx}}, \text{SNR}) &:= \limsup_{K \rightarrow \infty} \mathbb{E}[J_K^*(\{\gamma_t^k\})] = c + \text{tr}(S_\infty Q) \\ &+ \limsup_{K \rightarrow \infty} \frac{1}{K} \sum_{k=0}^{K-1} \text{tr} \left((A' S_\infty A - S_\infty + W) \mathbb{E}[P_{k|k-1}^k] \right) \quad (8) \end{aligned}$$

To find the optimal rate, we have to compute J_∞^* on each R^{tx} for the given SNR. Unfortunately, this is not possible because $\lim_{k \rightarrow \infty} \mathbb{E}[P_{k|k-1}^k]$ can not be computed in closed-form [32]. We therefore propose to consider computable upper bounds for it, which in turns allow us to compute upper bounds of the cost $J_\infty^*(R^{\text{tx}}, \text{SNR})$ for each transmission rate $R^{\text{tx}} = R_i$ and SNR.

First, we consider the scenario $R^{\text{tx}} = R^{\text{ctr}} = R_1$ and $\mathbf{P}[\gamma_{k-1}^k = 1] = \lambda(R_1, \text{SNR})$. As stated in [32], it holds that:

$$\lim_{k \rightarrow \infty} \mathbb{E}[P_{k|k-1}^k] \leq \bar{P}$$

where \bar{P} exists if $\lambda(R_1, \text{SNR}) > \bar{\lambda}_1$ and it can be found from:

$$\bar{P} = g_{\lambda(R_1, \text{SNR})}^T(\bar{P}).$$

Then we can bound the optimal LQG cost as:

$$\begin{aligned} J_\infty^*(R_1, \text{SNR}) &\leq \bar{J}_\infty^*(R_1, \text{SNR}) \\ \bar{J}_\infty^*(R_1, \text{SNR}) &= c + \text{tr}(S_\infty Q) + \text{tr}((A' S_\infty A + W - S_\infty) \bar{P}) \end{aligned}$$

The analysis becomes more involved when $R^{\text{tx}} = R_i = iR_1$ with $i > 1$. In this case it is not possible to find a single upper bound $\mathbb{E}[P_{k|k-1}^k] \leq \bar{P}$ for all k , but it is more meaningful to look for periodic upper bounds. In fact, measurements are transmitted only every i intervals, and therefore we expect to find an i -periodic sequence of bounds. More specifically, we will show that it is possible to find a set of i matrices $\{\bar{P}_j^i\}_{j=0}^{i-1}$ such that $\lim_{h \rightarrow \infty} \mathbb{E}[P_{ih+j|ih+j-1}^{ih+j}] \leq \bar{P}_j^i$. We will also show that \bar{P}_0^i can be computed as the fixed point of a Riccati-like operator that depends on the period $T_i = iT$ and $\lambda(R_i, \text{SNR})$, while \bar{P}_j^i can be computed from \bar{P}_0^i applying a suitable operator. This is summarized in the following theorem:

Theorem 4 *If $\lambda(R_i, \text{SNR}) > \bar{\lambda}_i$, then the optimal LQG cost can be upper-bounded by*

$$\bar{J}_\infty^*(R_i, \text{SNR}) = c + \text{tr}(S_\infty Q) + \frac{1}{i} \text{tr} \left((A' S_\infty A + W - S_\infty) \sum_{j=0}^{i-1} \bar{P}_j^i \right)$$

where

$$\begin{aligned} \bar{P}_0^i &= g_{\lambda(R_i, \text{SNR})}^{iT}(\bar{P}_0^i) \\ \bar{P}_j^i &= g_{\frac{j}{i}\lambda(R_i, \text{SNR})}^T(\bar{P}_0^i), \quad j = 1, \dots, i-1 \end{aligned}$$

PROOF. See Appendix A.

Finally, the optimal rate is chosen according to:

$$R^*(\text{SNR}) = \underset{R^{\text{tx}}}{\text{argmin}} \bar{J}_\infty^*(R^{\text{tx}}, \text{SNR}).$$

5 Sub-optimal solution for time-varying SNR

In the time-varying case, in order to optimally and simultaneously design the controller and the transmission rate, statistical information about the SNR dynamics is needed. However, even if this is available, the LQG framework would require the solution of a complex dynamic programming problem which might not be feasible. Moreover, due to the typical channel coherence time, SNR is not likely to change very rapidly as compared to the control period T , and therefore a quasi-static approach for the control rate could be effective. For this reason, we decide to fix the rate policy based on the static scenario. More specifically, at each transmission instant, the rate $R(k)$ to transmit y_k is selected to minimize the infinite-horizon LQG cost as if the SNR would remain constant and equal to the value of time instant k , denoted SNR_k :

$$R(k) = \operatorname{argmin}_{R^{\text{tx}}} \bar{J}_{\infty}^*(R^{\text{tx}}, SNR_k) \quad (9)$$

The solution is a static map that associates a transmission rate to each SNR, thus it can be implemented through a look-up table. From a practical point of view, a SNR measure can be provided by the Wi-Fi board while a specific user's routine can set the data-rate of the communication. It is worth mentioning that the possibility to set the data-rate is ensured by the Wi-Fi standard, and several off-the-shelf boards provide the SNR measure to the user. Alternatively it can be estimated e.g. from the RSSI. Practical considerations and execution times of the mentioned routine can be found in [4], while a similar implementation has been done in [34]. Note that $R(k)$ determines also the period until the following sent packet. Once the rate selection algorithm is chosen, we solve the LQG problem for the control and the estimate with time-varying SNR. From Theorem 3, the optimal control gain is not affected by SNR and R^{tx} , so it is the same with time-varying and constant SNR. Likewise, the optimal estimate procedure is the same given the information set, because a missing packet due to the adoption of a lower transmission rate is treated as a packet lost. It follows that the SRC under constant SNR can work in a time-varying SNR fashion just adding the time-varying on-line rate selection (see Fig. 3). It is interesting to note that, if the SNR is constant for a long period, the proposed solution coincides with the optimal solution for the constant SNR scenario without any modification.

Since the transmission rate can change, it is not more guaranteed that the closed-loop system is still stable since we are in the presence of a switching system, which is known to possibly be unstable even if the switching is performed between stable dynamics. In the following we prove the stability of the SRC with time-varying SNR. We consider that the SNR can be measured instantaneously by the sensor and it is able to select the optimal rate from the set $\{R_1, \dots, R_M\}$.

Assumption 5 *The sequence SNR_k is constant over each period $[Nh, Nh + N)$, with N the least common multiple of the first M positive integers, and lower-bounded by a given SNR_{\min} . Moreover, the first transmission is scheduled at $k = 0$.*

Piece-wise constant SNR_k with changes at multiples of N implies that the chosen rate is constant in the period $[Nh, Nh + N)$. Since N is multiple of any $i \in \{1, \dots, M\}$, $Nh + N$ is a transmission instant independently of which rate $R_i \in \{R_1, \dots, R_M\}$ has been chosen in $[Nh, Nh + N)$. This hypothesis is a technical assumption to simplify the subsequent analysis but it is reasonable if the SNR changes slowly, e.g. under slow fading scenario or with slow user mobility. Moreover, the lower bound SNR_{\min} excludes loss probabilities that would compromise stability even with a single rate approach. We consider the subsequence:

$$\left\{ \mathbb{E} \left[P_{Nh|Nh-1}^{Nh} \right] \right\}_{h=0}^{+\infty}.$$

A first issue is due to the fact that the evolution of the sequence above depends on the rate chosen in each period. The problem is even more difficult because, even for periods characterized by the same transmission rate, the arrival probability can vary within a certain range according to the SNR. Each transmission rate is so characterized by a worst case, that is in correspondence of the lowest SNR for which it is adopted:

$$SNR_{i,L} := \inf \{ SNR \geq SNR_{\min} : R^*(SNR) = R_i \}.$$

The corresponding limit arrival probability $\lambda_{i,L}$ for the transmission rate R_i is the arrival probability associated to $SNR_{i,L}$:

$$\lambda_{i,L} := \lambda(R_i, SNR_{i,L})$$

that is, under the mild hypothesis that the arrival probability is monotonically non-decreasing with respect to the SNR, the smallest arrival probability for which R_i is optimal. A graphical representation of this values is shown in Fig. 5 for a specific case.

Consider the linear operator:

$$\mathcal{L}^{T_i}(K, X) = (A_i + \lambda_{i,L}KC)X(A_i + \lambda_{i,L}KC)'$$

and its compositions¹:

$$\mathcal{L}_i(K, X) = \underbrace{\mathcal{L}^{iT} \circ \mathcal{L}^{iT} \circ \dots \circ \mathcal{L}^{iT}}_{N/i \text{ times}}(K, X)$$

Now we can state the stability theorem.

¹ with a little misuse of notation: $f \circ f(a, b) = f(a, f(a, b))$

Theorem 6 Consider that (A, B) is stabilizable and (A, \sqrt{W}) is detectable, while (A_i, C_i) is detectable and $(A_i, \sqrt{Q_i})$ is stabilizable $\forall i \in \{1, \dots, M\}$. Assume that Ass. (5) holds true with SNR_{\min} such that $\lambda_{i,L} > \bar{\lambda}_i \forall i$. Under rate adaptation law (9), SRC given in (7), and estimator given in (3)-(5), if there exist a \bar{K} and a $\bar{Y} > 0$ such that $\mathcal{L}_i(\bar{K}, \bar{Y}) < \bar{Y} \forall i$, then the closed-loop system is mean square stable.

PROOF. See Appendix B.

It is clear that a necessary condition for the stability of the time-varying case is the stability under constant SNR, which is guaranteed if $\lambda_{i,L} > \bar{\lambda}_i$: this motivates the condition on SNR_{\min} . The existence of \bar{K} and $\bar{Y} > 0$ is only a sufficient condition and possibly tighter conditions could exist. However, following the idea proposed in [32], the previous conditions can be cast into a semi-definite programming (SDP) problem, which can be numerically solved. In the interest of space, the SDP derivation is omitted.

6 Simulations

The results presented in the previous sections are now assessed within a specific simulation setup. First, we show the outcome of the rate selection algorithm for a particular case of study. Then, through the widely used Simulink-based TrueTime simulator [6], we implement the simplified but realistic network model introduced in Sec. 2 to show the benefits of the proposed scheme.

The system used for our simulation tests is a two-wheeled balancing robot, usually referred to as segway, consisting of a rigid body equipped with two wheels. Two DC motors provide the torque to the wheels aiming to keep the rigid body upright while moving on the plane. For sake of simplicity, we assume that the segway can move only along a straight line (i.e. the two DC motors are always supplied by the same voltage input). An inertial measurement sensor estimating the tilt angle and an encoder on a wheel constitute the on-board sensing and encoding device. The dynamics can be described by a continuous-time non-linear model: for the case of this work, we consider the dynamical model studied in [2]. Our approach is oriented to linear continuous-time plants, so we consider the state-space system linearized in the neighborhood of the origin:

$$A_c = \begin{bmatrix} 0 & 0 & 1 & 0 \\ 0 & 0 & 0 & 1 \\ 0 & 43.57 & -3.81 & 3.41 \\ 0 & 55.22 & 1.97 & -2.25 \end{bmatrix} \quad B_c = \begin{bmatrix} 0 \\ 0 \\ 4.92 \\ -3.25 \end{bmatrix} \quad C_c = \begin{bmatrix} 1 & 0 \\ 0 & 1 \\ 0 & 0 \\ 0 & 0 \end{bmatrix}'$$

where the state consists of the wheel angle, the tilt angle, and their derivatives. The input is the voltage of the DC motors and the output is the measurements given by the encoder and the inertial measurement sensor. The other matrices presented in Sec. 2 are:

$$\sqrt{W_c} = \begin{bmatrix} 1 & 100 & 0 & 0 \end{bmatrix} \quad W_c = \sqrt{W_c}' \sqrt{W_c} \quad U_c = 1$$

$$\sqrt{Q_c} = \begin{bmatrix} 0 & 10^{-4} & 0 & 0 \end{bmatrix}' \quad Q_c = \sqrt{Q_c} \sqrt{Q_c}' \quad R = \begin{bmatrix} 10^{-9} & 0 \\ 0 & 10^{-6} \end{bmatrix}$$

For the simulations we have adopted the set of sampling periods $\{T, 2T, 3T\}$, where $T = 0.01s$, that are used to discretize the linear continuous system. From the sampling periods, it is possible to compute the transmission rates and the control rates. We associate R_1, R_2, R_3 to the data-rates 54, 36, 18 Mbit/s, respectively. For each transmission rate and for each SNR level we have adopted the arrival probabilities in Fig. 2.

6.1 Numerical results under constant SNR

In Fig. 4 we report the asymptotic costs for the case of the segway as given by the formulas of Theorem 4 with constant SNR. The plot reports the cost on the y-axis and the inverse of the SNR, denoted by SNR^{-1} , on the x-axis. Note that, with this notation, it holds that $SNR|_{dB} = -SNR^{-1}|_{dB}$. For each transmission rate, the asymptotic cost is computed over only a finite number of quantized levels (with step of 1 dB) and as long as it admits a steady-state value, i.e. $\lambda(R_i, SNR) > \bar{\lambda}_i$. We can see that the highest transmission rate achieves the minimum cost for good channel condition, corresponding to left part of the plot, thanks to the largest available information set. Decreasing the SNR, i.e. for larger values on the x-axis, communications with the highest transmission rate start to be affected by packet loss, while the other rates are still reliable. Accordingly, while the cost with R_2 is still constant, the cost with R_1 increases and eventually R_2 achieves the lowest cost. The same happens for lower SNR with R_2 and R_3 , that eventually becomes the optimal rate. For even worse channel conditions, also communications with R_3 are not reliable and the sufficient condition for the stability is not satisfied. In Fig. 5 we highlight the loss probability corresponding to the optimal rate. We see that the optimal rate is not always the one for which the loss probability is the lowest, but it is a trade-off between the arrival probability and the control performances.

6.2 TrueTime implementation

TrueTime is a simulator for networked and real-time control systems compatible with the well-known Simulink environment. It provides a custom block library containing a Kernel block and a Network block that can interact with other blocks in an unique Simulink model. The

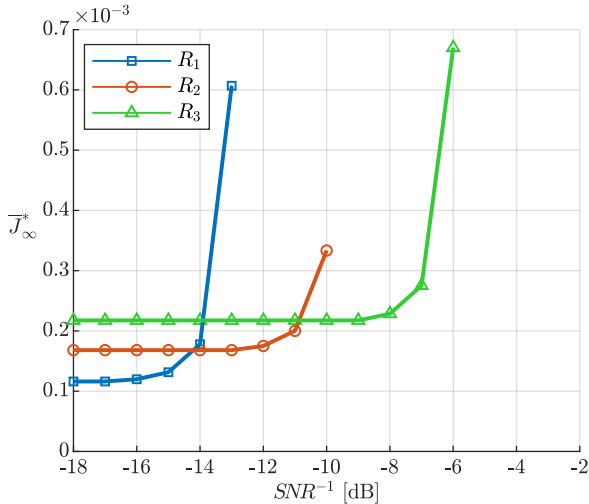


Fig. 4. LQG cost vs. SNR

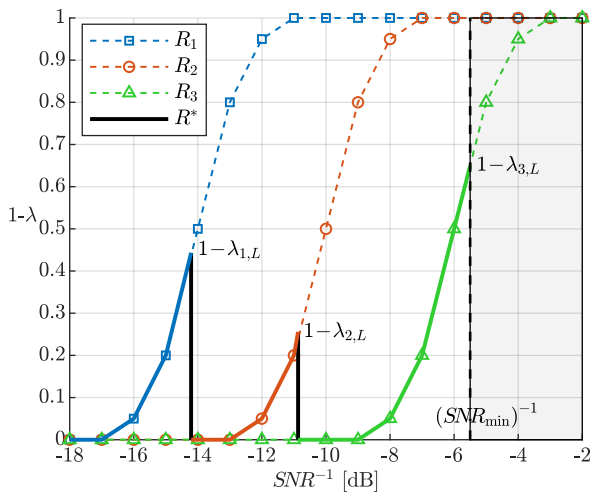


Fig. 5. Optimal loss probability

Kernel block models a computing processor with limited computational resources shared among multiple tasks, while the Network block models several widespread local networks like Ethernet, CAN, PROFINET, and ZigBee.

Our Simulink model comprises a block in which the dynamical non-linear system is implemented by a Matlab S-function, two Kernel blocks, and a IEEE 802.11b Network block that simulates the Wi-Fi communications between the two Kernel blocks. The input of the non-linear system is fed by the output of the first Kernel, which represents the control unit. It is the receiver in our setup. At each sampling time, it checks if new packets are arrived, then it elaborates the control input and provides it to the plant. The continuous-time output of the system is instead connected to the input of the second Kernel block, which represents the sensor. It is the transmitter in our setup. At the transmission instants indicated by the chosen rate, it packetizes and transmits

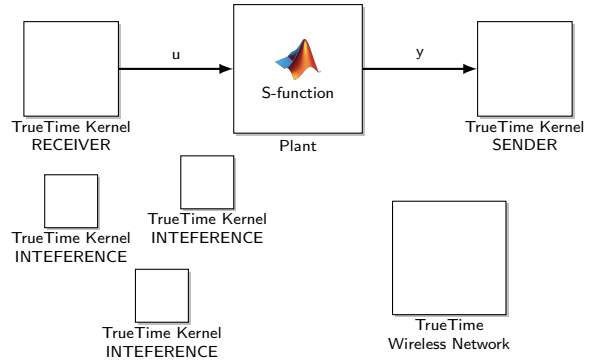


Fig. 6. TrueTime model (simplified)

the system output. The IEEE 802.11b Network block manages the communication from the sensor to the control unit and simulates the access to the medium, the transmission intervals, and the packet losses. Fig. 6 is an intuitive sketch of the implemented Simulink model. A set of Kernel blocks are used to simulate different levels of noise. Since TrueTime assumes a rather simplistic model of the bit error rate, it does not capture the behaviour of the packet loss probability due to the changing data-rate, so we decide to modify the source files of the simulator in order to include the behavior of Fig. 2.

6.3 Numerical results under time-varying SNR

It is interesting to compare our control strategy to existing controllers for NCSs. One popular approach [23] [9], sometimes referred to as *emulation-based*, considers to design the regulator as if the network is not present, while, in the implementation, a lost packet is replaced by the last received one. This approach is attractive because it allows to re-use the standard well-known control schemes. Since any possible control algorithm can be adopted according to this strategy, we decide to consider a standard Kalman filter followed by the optimal control gain. We will refer to it as *emulation-based LQG controller*. We aim to compare the proposed cross-layer approach to the independent design of network and control, e.g. when the future channel condition is optimistically considered or when the chosen rate is conservative.

The SRC can switch R^{tx} among R_1 , R_2 , and R_3 , while R^{ctr} is fixed to R_1 accordingly. The emulation-based controller is not designed to support a control rate different from the transmission rate, so $R^{tx} = R^{ctr}$. We decide to consider a first controller with R_1 and a second one with R_3 . In particular, rate R_1 should provide high performances when the communication channel is good, while R_3 would provide lower performances but a greater robustness when the channel quality degrades. In every controller we add integral action for tracking of step reference on the wheel angle. In our simulations, we consider a square wave with period 12s and duty cycle

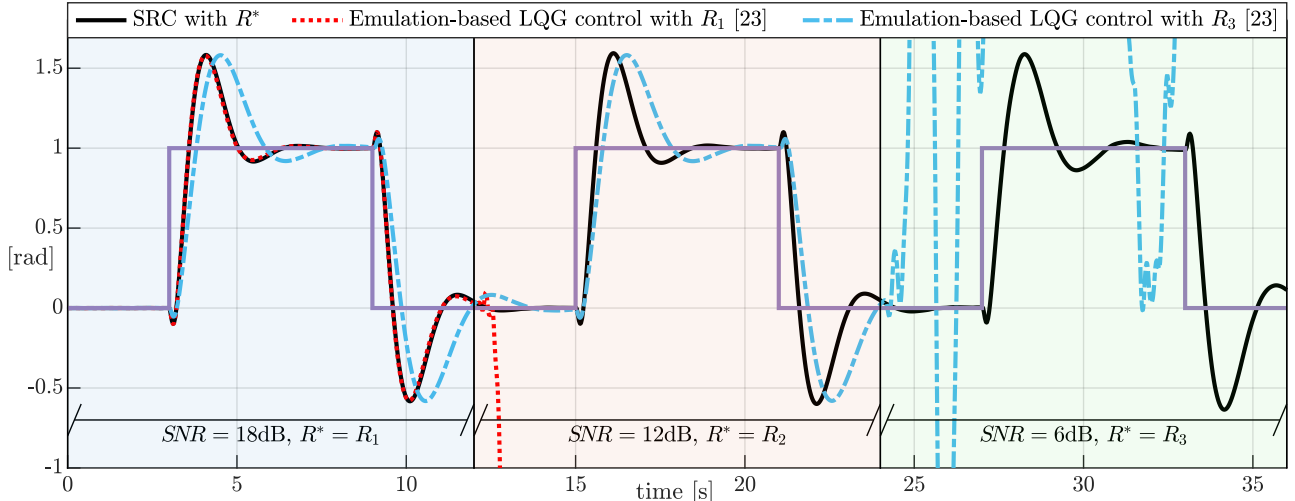


Fig. 7. Comparison on the square wave response between SRC and emulation-based LQG controller [23].

50%. We consider a piece-wise constant SNR:

$$SNR(t) = \begin{cases} 18 \text{ dB} & t \in [0\text{s}, 12\text{s}) \\ 12 \text{ dB} & t \in [12\text{s}, 24\text{s}) \\ 6 \text{ dB} & t \in [24\text{s}, 36\text{s}) \end{cases}$$

that represents the case in which the channel is ideal in the first period ($R^* = R_1$), then it deteriorates in the second period ($R^* = R_2$), and finally it is affected by high noise ($R^* = R_3$). The results are plotted in Fig. 7. In the first period, with high SNR, the SRC and the emulation-based LQG controller with R_1 coincide. They outperform the emulation-based LQG controller with R_3 that exhibits a longer settling time due to the longer sampling period. Note that, in this period, emulation-based step response with R_3 would coincide to the output with a model-based controller identical to SRC but with $R^{\text{ctr}} = R^{\text{tx}} = R_3$, so it is possible to infer the improvement achieved by the adoption of a higher rate also with respect to the same control algorithm. In the second period, the SNR decreases and the emulation-based LQG controller with R_1 is not able to stabilize the system due to the high packet loss incurred ($\lambda(R_1, 12 \text{ dB}) = 0.95$). The emulation-based LQG controller with R_3 obtains exactly the same result of the previous period, because the changing of SNR from 18 dB to 12 dB is invisible for R_3 since the corresponding packet loss probabilities are both zero (see Fig. 5). The SRC switches from R_1 and R_2 but its performance is barely affected by this change. In the third period, where the noise is high, the emulation-based LQG controller with R_3 becomes unstable. Also the performances of the SRC deteriorate due to the severe packet loss (settling time 0.5 s worse). However, the degradation is mild if we take into account that the SRC with $R^{\text{tx}} = R_1$ or with $R^{\text{tx}} = R_2$ would work without feedback due to the very high loss probabilities for such a SNR (see Fig. 5) and would not be able to stabilize the system. It is possible to see the benefits of the pro-

posed rate adaptation mechanism: under good channel conditions, an high R^{tx} is adopted ensuring better performance than a lower one, while, in bad channel conditions, a low R^{tx} guarantees good performances when an higher one may led to instability. These simulations clearly show the benefit of a model-based control design to take into account packet losses with respect to the the emulation-based approach.

7 Conclusions and future works

This work analyses the LQG control for a NCS where the link between the sensor and the controller is implemented through a Wi-Fi network. Based on the relationship between the packet error probability and the SNR, we study the rate selection algorithm that minimizes the LQG cost under constant SNR. We show that the optimal rate increases with the SNR, as expected, however under some specific values of SNR, the rate selection algorithm dictates to pick a fast rate with non-negligible packet loss probability (up to 50%) rather than a lower rate with minimal packet loss. Adopting an higher update rate of the input with respect to the sampling rate of the output, we provide the control strategies named SRC that is optimal with constant rate (i.e. constant SNR) and is guaranteed, under mild conditions, to stabilize the system also in time-varying channel conditions (i.e. time-varying SNR). Numerical simulations involving TrueTime simulator show the benefits of the adaptive approach under a time-varying SNR condition with respect to standard constant-rate controller. The proposed algorithm can be further generalized to include multi-agent systems, and possible applications are collaborative robotics, building maintenance, and formation control of swarm of autonomous systems. The next step, starting from the implementation presented in [5], is to experimentally validate the proposed algorithm.

A Proofs for constant SNR

First we introduce the following lemma.

Lemma 7 *The following properties hold:*

- (1) $g_{\lambda}^{\tau'+\tau''}(P) = g_0^{\tau'} \circ g_{\lambda}^{\tau''}(P) \forall \tau', \tau'' > 0$.
- (2) Consider $X \leq Y$. Then $g_{\lambda}^{\tau}(X) \leq g_{\lambda}^{\tau}(Y)$.
- (3) Consider $\lambda' \leq \lambda''$. Then $g_{\lambda'}^{\tau}(P) \geq g_{\lambda''}^{\tau}(P)$.
- (4) Consider $X, Y \geq 0$ and $\alpha \in [0, 1]$. Then $g_{\lambda}^{\tau}(\alpha X + (1-\alpha)Y) \geq \alpha g_{\lambda}^{\tau}(X) + (1-\alpha)g_{\lambda}^{\tau}(Y)$.
- (5) Consider λ', λ'' and $\alpha \in [0, 1]$. Then $g_{\alpha\lambda'+(1-\alpha)\lambda''}^{\tau}(X) = \alpha g_{\lambda'}^{\tau}(X) + (1-\alpha)g_{\lambda''}^{\tau}(X)$.
- (6) Let $X \geq 0$ be a random matrix. Then $\mathbb{E}[g_{\lambda}^{\tau}(X)] \leq g_{\lambda}^{\tau}(\mathbb{E}[X])$.

PROOF. (1) can be proved by computing $g_0^{\tau'} \circ g_{\lambda}^{\tau''}(P)$ and using the definitions given in Sec. 2, under the key assumption that R is independent of the sampling period. Properties (2)-(4) are given in [32], while (5) is trivial. They state that $g_{\lambda}^{\tau}(X)$ is monotonically increasing w.r.t. X , monotonically decreasing w.r.t. λ , concave w.r.t. X , and affine w.r.t. λ , respectively. (6) follows immediately from (4) employing Jensen's inequality.

Consider $R^{\text{ctr}} = R_1$ and $R^{\text{tx}} = R_i$. Without loss of generality, we assume that only the output at time instants ih , $h \in \mathbb{N}$ is sent, while the output at other instants is never sent. Recalling that the measurement y_{ih} arrives in the time interval $(ih, ih+i)$ or it never arrives, we can summarize:

$$\begin{aligned} \gamma_{ih}^{ih+i+n} &= \gamma_{ih}^{ih+i} \quad \forall n \in \mathbb{N} \\ \gamma_{ih+j}^{ih+j+n} &= 0 \quad j \in \{1, \dots, i-1\}, \forall n \in \mathbb{N}. \end{aligned}$$

Lemma 8 *The error covariance on the transmission instants with $R^{\text{ctr}} = R_1$ and $R^{\text{tx}} = R_i$ has the same evolution of the case with $R^{\text{tx}} = R^{\text{ctr}} = R_i$, i.e.:*

$$P_{ih|ih-1}^{ih} = g_{\gamma_{ih-i}}^{iT} \left(P_{ih-i|ih-i-1}^{ih-i} \right).$$

PROOF. For sake of simplicity, we prove the Lemma with $R^{\text{tx}} = R_2$ and even time instants as transmission instants. By Eq. (5), it holds that:

$$\begin{aligned} P_{2h|2h-1}^{2h} &= g_{\gamma_{2h-1}}^T \left(P_{2h-1|2h-2}^{2h} \right) \\ P_{2h-1|2h-2}^{2h} &= g_{\gamma_{2h-2}}^T \left(P_{2h-2|2h-3}^{2h} \right) \end{aligned}$$

and so

$$P_{2h|2h-1}^{2h} = g_{\gamma_{2h-1}}^T \circ g_{\gamma_{2h-2}}^T \left(P_{2h-2|2h-3}^{2h} \right).$$

Moreover, $P_{2h-2|2h-3}^{2h} = P_{2h-2|2h-3}^{2h-2}$ because \mathcal{I}_{2h} does not have more information than \mathcal{I}_{2h-2} that is useful for computing $\{\hat{x}_{k|k-1}^{2h}\}_{k=0}^{2h-2}$, since if the measurement does not arrive until the next transmission instant it is discarded. By hypothesis $\gamma_{2h-1}^{2h} = 0$. We obtain:

$$\begin{aligned} P_{2h|2h-1}^{2h} &= g_0^T \circ g_{\gamma_{2h-2}}^T \left(P_{2h-2|2h-3}^{2h-2} \right), \\ &= g_{\gamma_{2h-2}}^{2T} \left(P_{2h-2|2h-3}^{2h-2} \right) \end{aligned}$$

using Lemma 7(1).

Lemma 9 *Consider the arrival instant of y_{ih} is uniformly distributed across the period $(ih, ih+i)$. The arrival process is then described by:*

$$\mathbf{P}[\gamma_{ih}^{ih+j} = 1] = \frac{j}{i} \lambda(R_i, \text{SNR}) = \frac{j}{i} \lambda_i \quad j \in \{1, \dots, i\}$$

It is schematically depicted in Fig. A.1. Then, the expected error covariance can be upper-bounded by:

$$\mathbb{E} \left[P_{k|k-1}^k \right] \leq \bar{P}_{k|k-1}^k \quad \forall k \in \mathbb{N}$$

where for $k = ih$:

$$\bar{P}_{ih|ih-1}^{ih} = g_{\lambda_i}^{iT} \left(\bar{P}_{ih-i|ih-i-1}^{ih-i} \right) \quad \bar{P}_{0|-1}^0 = \mathbb{E} \left[P_{0|-1}^0 \right]$$

while for $k = ih+j$, $j \in \{1, \dots, i-1\}$:

$$\bar{P}_{ih+j|ih+j-1}^{ih+j} = g_{\frac{j}{i}\lambda_i}^{jT} \left(\bar{P}_{ih|ih-1}^{ih} \right)$$

PROOF. We prove the lemma for the case $R^{\text{tx}} = R_2$. The upper bound on even instants follows from [32] taking into account that on even instants the error covariance has the same evolution of the case with $R^{\text{tx}} = R^{\text{ctr}} = R_2$, as shown in Lemma 8. For odd instants:

$$\begin{aligned} \mathbb{E} \left[P_{2h+1|2h}^{2h+1} \right] &= \mathbb{E} \left[g_{\gamma_{2h+1}}^T \left(P_{2h|2h-1}^{2h} \right) \right] \\ &= \mathbb{E} \left[g_{\frac{\lambda_2}{2}}^T \left(P_{2h|2h-1}^{2h} \right) \right] \\ &\leq g_{\frac{\lambda_2}{2}}^T \left(\mathbb{E} \left[P_{2h|2h-1}^{2h} \right] \right) \\ &\leq g_{\frac{\lambda_2}{2}}^T \left(\bar{P}_{2h|2h-1}^{2h} \right) = \bar{P}_{2h+1|h}^{2h+1} \end{aligned}$$

where we have employed the fact $g_{\gamma}^T(X)$ is affine w.r.t γ , it is concave w.r.t. X and Jensen's inequality, and that it is monotonically increasing w.r.t. X , as stated in Lemma 7(2)-(6).

PROOF (Theorem 4). For sake of simplicity we restrict to the case $R^{\text{tx}} = R_2$. If $\lambda_2 > \bar{\lambda}_2$, it has been

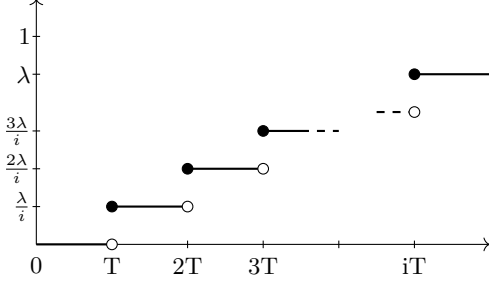


Fig. A.1. Arrival probability within two transmission instants

proved in [32] that the sequence of upper bounds given in Lemma 9 on even instants converges:

$$\lim_{h \rightarrow \infty} \bar{P}_{2h|2h-1}^2 = \bar{P}_0^2 \quad \text{with} \quad \bar{P}_0^2 = g_{\lambda_2}^{2T}(\bar{P}_0^2).$$

It follows that the upper bound on odd instants at steady-state is:

$$\bar{P}_1^2 = g_{\lambda_2}^T(\bar{P}_0^2).$$

We can divide the cost (8) in two parts:

$$\begin{aligned} J_\infty^*(R_2, SNR) &= c + \text{tr}(S_\infty Q) \\ &+ \limsup_{K \rightarrow \infty} \frac{1}{K} \sum_{\substack{k=0, \\ \text{even}}}^{K-1} \text{tr} \left((A' S_\infty A - S_\infty + W) \mathbb{E}[P_{k|k-1}^k] \right) \\ &+ \limsup_{K \rightarrow \infty} \frac{1}{K} \sum_{\substack{k=0, \\ \text{odd}}}^{K-1} \text{tr} \left((A' S_\infty A - S_\infty + W) \mathbb{E}[P_{k|k-1}^k] \right). \end{aligned}$$

Since $A' S_\infty A - S_\infty + W \geq 0$, the cost is upper-bounded by substituting the limsup of the expected error covariance on even and odd instants with the corresponding steady-state upper bounds. Then, the statement of the theorem follows immediately.

B Proofs for time-varying SNR

In this section, to simplify the notation, the one-step prediction error covariance matrix at the time instant k is denoted by P_k , i.e.: $P_k := P_{k|k-1}^k$.

Based on the operator $g_\lambda^T(X)$, we define following non-linear operators:

$$g_i(X) = \underbrace{g_{\lambda_{i,L}}^{iT} \circ g_{\lambda_{i,L}}^{iT} \circ \dots \circ g_{\lambda_{i,L}}^{iT}}_{N/i \text{ times}}(X)$$

Note that the subscript indicates both the sampling period and the limit arrival probability.

Define the operator:

$$\Phi_\lambda^{Ti}(K, X) = \lambda(F_i X F_i' + V_i) + (1 - \lambda)(A_i X A_i' + Q_i)$$

with $F_i = A_i + KC$, $V_i = Q_i + K R K'$, where T_i is the sampling period with which A_i and Q_i are discretized. It is affine with respect to the second argument. Define the following operators:

$$\Phi_i(K, X) = \underbrace{\Phi_{\lambda_{i,L}}^{iT} \circ \Phi_{\lambda_{i,L}}^{iT} \circ \dots \circ \Phi_{\lambda_{i,L}}^{iT}}_{N/i \text{ times}}(K, X)$$

Note that K is always the same from the inner to the outer application of the operator and, as for $g_i(\cdot)$, the subscript denotes both the sampling period and the limit arrival probability. They are still affine because the composition of affine operators is an affine operator. For each affine operator there exists a linear operator such that the affine operator can be obtained by the sum of the linear operator and a constant. Hence, it is possible to define:

$$\mathcal{L}_i(K, X) : \Phi_i(K, X) = \mathcal{L}_i(K, X) + U_i$$

Note that these operators correspond to the ones given in Eq. (5). Finally, consider:

$$\bar{\Phi}_i(K, X) = \mathcal{L}_i(K, X) + \bar{U}$$

where $\bar{U} \geq 0$ is such that $\bar{U} \geq U_i \forall i \in \{1, \dots, M\}$. It is easy to prove that it always exists. Now we recall some important properties that hold for the previous operators.

Lemma 10 *The following properties hold:*

- (1) Consider $X \geq 0$. Then $g_\lambda^{Ti}(X) \leq \Phi_\lambda^{Ti}(K, X) \forall K \forall i$.
- (2) Consider $X \geq 0$. Then $g_i(X) \leq \Phi_i(K, X) \forall K \forall i$.

PROOF. (1) is given in [32], while (2) is a consequence of (1) and Lemma 7(2).

Lemma 11 *Consider a generic sequence $\{i_k\}$ with $i_k \in \{1, \dots, M\}$. If there exist a \bar{K} and a $\bar{Y} > 0$ such that $\mathcal{L}_i(\bar{K}, \bar{Y}) < \bar{Y} \forall i \in \{1, \dots, M\}$, then the sequence $Y_{k+1} = \bar{\Phi}_{i_k}(\bar{K}, Y_k)$ is bounded $\forall Y_0 \geq 0$.*

PROOF. The following properties hold:

- (1) $\forall Y_0 \geq 0 \exists m_{Y_0} : Y_0 \leq m_{Y_0} \bar{Y}$,
- (2) $\exists m_{\bar{Y}} : \bar{U} \leq m_{\bar{Y}} \bar{Y}$,
- (3) $\forall i \exists r_i \in (0, 1) : \mathcal{L}_i(\bar{K}, \bar{Y}) < r_i \bar{Y}$,
- (4) $r = \max(r_i) \Rightarrow r \in (0, 1), \mathcal{L}_i(\bar{K}, \bar{Y}) < r \bar{Y} \forall i$.

Choose a generic initial condition $Y_0 \geq 0$. It holds that:

$$\begin{aligned}
Y_{k+1} &= \bar{\Phi}_{i_k} \circ \bar{\Phi}_{i_{k-1}} \circ \dots \circ \bar{\Phi}_{i_0}(\bar{K}, Y_0) \\
&= \mathcal{L}_{i_k} \circ \mathcal{L}_{i_{k-1}} \circ \dots \circ \mathcal{L}_{i_0}(\bar{K}, Y_0) \\
&\quad + \sum_{t=1}^k \mathcal{L}_{i_k} \circ \mathcal{L}_{i_{k-1}} \circ \dots \circ \mathcal{L}_{i_t}(\bar{K}, \bar{U}) + \bar{U} \\
&\leq m_{Y_0} \mathcal{L}_{i_k} \circ \mathcal{L}_{i_{k-1}} \circ \dots \circ \mathcal{L}_{i_0}(\bar{K}, \bar{Y}) \\
&\quad + m_{\bar{U}} \left(\sum_{t=1}^k \mathcal{L}_{i_k} \circ \mathcal{L}_{i_{k-1}} \circ \dots \circ \mathcal{L}_{i_t}(\bar{K}, \bar{Y}) + \bar{Y} \right) \\
&\leq m_{Y_0} r^k \bar{Y} + m_{\bar{U}} \sum_{t=0}^k r^t \bar{Y} \leq \left(m_{Y_0} + \frac{m_{\bar{U}}}{1-r} \right) \bar{Y}
\end{aligned}$$

where we exploit Lemma 10 and the linearity of \mathcal{L} .

Consider the following sequence of matrices:

$$\bar{P}_{Nh+N} = g_{i_{Nh}}(\bar{P}_{Nh}) \quad \bar{P}_0 = P_0.$$

Lemma 12 Consider a generic sequence of $SNR_{Nh} \geq SNR_{\min}$ and the corresponding sequence of indexes of optimal rates $\{i_{Nh}\}$ according to the rate selection algorithm (9). If there exist a \bar{K} and an $\bar{Y} > 0$ such that $\mathcal{L}_i(\bar{K}, \bar{Y}) < \bar{Y} \forall i$, then:

- (1) $\exists M \geq 0 : \bar{P}_{Nh} < M \forall h$
- (2) $\mathbb{E}[P_{Nh}] \leq \bar{P}_{Nh} \forall h$
- (3) $\exists \bar{M} \geq 0 : \mathbb{E}[P_k] < \bar{M} \forall k$.

PROOF. Consider the sequence of the upper-upper-bounds:

$$\begin{aligned}
\bar{P}_{Nh+N} &= g_{i_{Nh}}(\bar{P}_{Nh}) \\
&\leq \Phi_{i_{Nh}}(\bar{K}, \bar{P}_{Nh}) \\
&= \mathcal{L}_{i_{Nh}}(\bar{K}, \bar{P}_{Nh}) + U_{i_{Nh}} \\
&\leq \mathcal{L}_{i_{Nh}}(\bar{K}, \bar{P}_{Nh}) + \bar{U} \\
&= \bar{\Phi}_{i_{Nh}}(\bar{K}, \bar{P}_{Nh})
\end{aligned}$$

where we have exploited the definitions of \bar{P} , \mathcal{L} , $\bar{\Phi}$ and Lemma 10. Now consider the sequence $\hat{P}_{Nh} = \bar{\Phi}_{i_{Nh}}(\hat{P}_{Nh-N})$ starting from P_0 . This sequence is bounded according to Lemma 11 and it limits the sequence of upper-upper-bounds: this proves the first claim.

The second claim can be proved by induction. It holds for $h = 0$ since $\bar{P}_0 = P_0 = \mathbb{E}[P_0]$. Now assume that $\mathbb{E}[P_{Nh-N}] \leq \bar{P}_{Nh-N}$. If SNR_{Nh} is such that the optimal

transmission rate is R_i and the arrival probability is λ_i , we have:

$$\begin{aligned}
\mathbb{E}[P_{Nh}] &\leq \underbrace{g_{\lambda_i}^{iT} \circ g_{\lambda_i}^{iT} \circ \dots \circ g_{\lambda_i}^{iT}}_{N/i \text{ times}}(\mathbb{E}[P_{Nh-N}]) \\
&\leq \underbrace{g_{\lambda_{i,L}}^{iT} \circ g_{\lambda_{i,L}}^{iT} \circ \dots \circ g_{\lambda_{i,L}}^{iT}}_{N/i \text{ times}}(\mathbb{E}[P_{Nh-N}]) \leq \bar{P}_{Nh}
\end{aligned}$$

where the first inequality holds for Lemma 7(6) and the second holds for Lemma 7(3), as long as $\lambda_i \geq \lambda_{i,L}$, true by definition of $\lambda_{i,L}$ if $SNR \geq SNR_{\min}$.

The third claim follows immediately from the first two claims (for $k = Nh$) and the fact that the error covariance can not diverge in a finite number of steps (for $k \in \{Nh + 1, \dots, Nh + N - 1\}$).

PROOF (Theorem 6). Under the hypothesis of (A, B) stabilizable and (A, \sqrt{W}) detectable, the system is mean square stable if the cost is bounded. Consider the asymptotic cost:

$$\begin{aligned}
J_{\infty}^* &= c + \text{tr}(S_{\infty}Q) \\
&+ \limsup_{K \rightarrow \infty} \frac{1}{K} \sum_{k=0}^{K-1} \text{tr} \left((A'S_{\infty}A - S_{\infty} + W) \mathbb{E}[P_{k|k-1}^k] \right)
\end{aligned}$$

where the steady-state value S_{∞} exists under the hypothesis of (A, B) stabilizable and (A, \sqrt{W}) detectable. Since there exist a \bar{K} and a $\bar{Y} > 0$ such that $\mathcal{L}_i(\bar{K}, \bar{Y}) < \bar{Y} \forall i$ and $SNR_k \geq SNR_{\min}$, the sequence of expected error covariance is bounded $\mathbb{E}[P_{k|k-1}^k] \leq \bar{M}$ according to Lemma 12. It immediately follows that:

$$\begin{aligned}
J_{\infty}^* &\leq c + \text{tr}(S_{\infty}Q) \\
&\quad + \limsup_{K \rightarrow \infty} \frac{1}{K} \sum_{k=0}^{K-1} \text{tr} \left((A'S_{\infty}A - S_{\infty} + W) \bar{M} \right) \\
&= c + \text{tr}(S_{\infty}Q) + \text{tr} \left((A'S_{\infty}A - S_{\infty} + W) \bar{M} \right).
\end{aligned}$$

The right hand side is bounded, that implies that also the left hand side is bounded, which concludes the proof.

References

- [1] Brian DO Anderson and John B Moore. Optimal filtering. *Englewood Cliffs*, 21, 1979.
- [2] Riccardo Antonello and Luca Schenato. Laboratory activity 4: Longitudinal state-space control of the balancing robot. Accessed: November 2019. http://automatica.dei.unipd.it/t1_files/utenti/lucaschenato/SEGWAY_GUIDE.pdf.
- [3] Saad Biaz and Shaoen Wu. Rate adaptation algorithms for IEEE 802.11 networks: A survey and comparison. In *2008 IEEE Symposium on Computers and Communications (ISCC)*, pages 130–136. IEEE, 2008.

- [4] Francesco Branz, Riccardo Antonello, Federico Tramarin, Tommaso Fedullo, Stefano Vitturi, and Luca Schenato. Embedded systems for time-critical applications over Wi-Fi: design and experimental assessment. In *2019 IEEE International Conference on Industrial Informatics (INDIN)*, 2019.
- [5] Francesco Branz, Matthias Pezzutto, Riccardo Antonello, Federico Tramarin, and Luca Schenato. Drive-by-Wi-Fi: testing 1 kHz control experiments over wireless. In *2019 European Control Conference (ECC)*, pages 2990–2995. IEEE, 2019.
- [6] Anton Cervin, Dan Henriksson, Bo Lincoln, Johan Eker, and Karl-Erik Arzen. How does control timing affect performance? Analysis and simulation of timing using Jitterbug and TrueTime. *IEEE Control Systems Magazine*, 23(3):16–30, 2003.
- [7] Jeremy Colandairaj, George W Irwin, and William Scanlon. Wireless networked control systems with QoS-based sampling. *IET Control Theory & Applications*, 1(1):430–438, 2007.
- [8] Patrizio Colaneri and Giuseppe De Nicolao. Multirate LQG control of continuous-time stochastic systems. *Automatica*, 31(4):591–596, 1995.
- [9] Dragan B Dačić and Dragan Nešić. Quadratic stabilization of linear networked control systems via simultaneous protocol and controller design. *Automatica*, 43(7):1145–1155, 2007.
- [10] Feng Ding and Tongwen Chen. Combined parameter and output estimation of dual-rate systems using an auxiliary model. *Automatica*, 40(10):1739–1748, 2004.
- [11] FieldComm Group. HART Protocol Specification. <https://fieldcommgroup.org/hart-specifications>. Accessed: November 2019.
- [12] Eloy Garcia and Panos Antsaklis. Model-based control of networked distributed systems with multi-rate state feedback updates. *International Journal of Control*, 86(9):1503–1517, 2013.
- [13] Gavin Holland, Nitin Vaidya, and Paramvir Bahl. A rate-adaptive MAC protocol for multi-hop wireless networks. In *2001 International Conference on Mobile Computing and Networking*, pages 236–251. ACM, 2001.
- [14] International Society of Automation (ISA). ANSI/ISA-100.11a-2011 Wireless systems for industrial automation: Process control and related applications. <https://www.isa.org/store/products/product-detail/?productId=118261>. Accessed: November 2019.
- [15] Ad Kamerman and Leo Monteban. Wavelan®-ii: A high-performance wireless LAN for the unlicensed band. *Bell Labs Technical Journal*, 2(3):118–133, 1997.
- [16] Teemu Karhima, Aki Silvennoinen, Michael Hall, and Sven G Haggman. IEEE 802.11 b/g WLAN tolerance to jamming. In *2004 Military Communications Conference (MILCOM)*, volume 3, pages 1364–1370. IEEE, 2004.
- [17] Mathieu Lacage, Mohammad Hossein Manshaei, and Thierry Turletti. IEEE 802.11 rate adaptation: A practical approach. In *2004 ACM International Symposium on Modeling, Analysis and Simulation of Wireless and Mobile Systems*, pages 126–134. ACM, 2004.
- [18] Jay H Lee and Manfred Morari. Robust inferential control of multi-rate sampled-data systems. *Chemical Engineering Science*, 47(4):865–885, 1992.
- [19] Frank L Lewis, Lihua Xie, and Dan Popa. *Optimal and robust estimation: with an introduction to stochastic control theory*. CRC press, 2017.
- [20] Dongguang Li, Sirish L Shah, and Tongwen Chen. Analysis of dual-rate inferential control systems. *Automatica*, 38(6):1053–1059, 2002.
- [21] Weiping Lu and Grant D Fisher. Output estimation with multi-rate sampling. *International Journal of Control*, 48(1):149–160, 1988.
- [22] Girish N Nair, Fabio Fagnani, Sandro Zampieri, and Robin J Evans. Feedback control under data rate constraints: An overview. *Proceedings of the IEEE*, 95(1):108–137, 2007.
- [23] Dragan Nešić and Andrew R Teel. Input-to-state stability of networked control systems. *Automatica*, 40(12):2121–2128, 2004.
- [24] Pangun Park, José Araújo, and Karl Henrik Johansson. Wireless networked control system co-design. In *2011 International Conference on Networking, Sensing and Control*, pages 486–491, 2011.
- [25] Pangun Park, Piergiuseppe Di Marco, Carlo Fischione, and Karl Henrik Johansson. Modeling and optimization of the IEEE 802.15.4 protocol for reliable and timely communications. *IEEE Transactions on Parallel and Distributed Systems*, 24(3):550–564, 2012.
- [26] Pangun Park, Sinem Coleri Ergen, Carlo Fischione, Chenyang Lu, and Karl Henrik Johansson. Wireless network design for control systems: A survey. *IEEE Communications Surveys & Tutorials*, 20(2):978–1013, 2018.
- [27] Stig Petersen and Simon Carlsen. WirelessHART vs. ISA100.11a: The Format War Hits the Factory Floor. *IEEE Industrial Electronics Magazine*, 5(4):23–34, Dec 2011.
- [28] Matthias Pezzutto, Federico Tramarin, Subhrakanti Dey, and Luca Schenato. SNR-triggered Communication Rate for LQG Control over Wi-Fi. In *2018 IEEE Conference on Decision and Control (CDC)*, pages 1725–1730. IEEE, 2018.
- [29] Abusayeed Saifullah, Chengjie Wu, Paras Babu Tiwari, You Xu, Yong Fu, Chenyang Lu, and Yixin Chen. Near optimal rate selection for wireless control systems. *ACM Transactions on Embedded Computing Systems*, 13(4s):128, 2014.
- [30] Luca Schenato. Optimal estimation in networked control systems subject to random delay and packet drop. *IEEE Transactions on Automatic Control*, 53(5):1311–1317, 2008.
- [31] Luca Schenato, Bruno Sinopoli, Massimo Franceschetti, Kameshwar Poolla, and Shankar S Sastry. Foundations of control and estimation over lossy networks. *Proceedings of the IEEE*, 95(1):163–187, 2007.
- [32] Bruno Sinopoli, Luca Schenato, Massimo Franceschetti, Kameshwar Poolla, Michael I Jordan, and Shankar S Sastry. Kalman filtering with intermittent observations. *IEEE Transactions on Automatic Control*, 49(9):1453–1464, 2004.
- [33] Bernard Sklar and Fredric J Harris. *Digital communications: fundamentals and applications*, volume 2001. Prentice-hall Englewood Cliffs, NJ, 1988.
- [34] Federico Tramarin, Stefano Vitturi, and Michele Luvisotto. A dynamic rate selection algorithm for IEEE 802.11 industrial wireless LAN. *IEEE Transactions on Industrial Informatics*, 13(2):846–855, 2017.
- [35] Federico Tramarin, Stefano Vitturi, Michele Luvisotto, and Andrea Zanella. On the use of IEEE 802.11n for industrial communications. *IEEE Transactions on Industrial Informatics*, 12(5):1877–1886, 2016.
- [36] Stefano Vitturi, Lucia Seno, Federico Tramarin, and Matteo Bertocco. On the rate adaptation techniques of IEEE 802.11 networks for industrial applications. *IEEE Transactions on Industrial Informatics*, 9(1):198–208, 2013.

- [37] Yi-Hung Wei, Quan Leng, Song Han, Aloysius K Mok, Wenlong Zhang, and Masayoshi Tomizuka. RT-WiFi: Real-time high-speed communication protocol for wireless cyber-physical control applications. In *2013 IEEE Real-Time Systems Symposium (RTSS)*, pages 140–149. IEEE, 2013.
- [38] Dong Xia, Jonathan Hart, and Qiang Fu. Evaluation of the Minstrel rate adaptation algorithm in IEEE 802.11 g WLANs. In *2013 IEEE International Conference on Communications (ICC)*, pages 2223–2228. IEEE, 2013.